Eur Biophys J (1985) 12: 129–142

European Biophysics Journal

Rate theoretical analysis of ion-selectivity in membrane channels with elastically bound ligands

H. Schröder

Fakultät für Physik, Universität Konstanz, D-7750 Konstanz, Federal Republic of Germany

Received December 28, 1984/Accepted February 28, 1985

Abstract. This article demonstrates why a gramicidin-like pore features ion-specific conductivity with the sequence $Cs^+ > Rb^+ > K^+ > Na^+ > Li^+$. The starting point is a generalized transition state method for escape across multi-dimensional barriers. This model-independent procedure provides an adequate description of the transport process for ions along the interior of a channel-like molecule with flexible ligands. Moreover, the proper treatment of three-dimensional motion of ions within the channel allows for a cross-coupling with the ligands' motion. It is shown that the particle migrating along a sequence of binding sites actually corresponds to a polaron, where the individual dwelling times strongly depend on the ion's radius.

Key words: Ion – channel interaction, polarization, rate theory, ion transport, conductivity sequences

Introduction

The passive transport of alkali ions through membrane pores is a very complex process and is only fairly well understood in certain simple cases, where the structure of the pore forming molecule is known, as is the case for gramicidin A (Urry et al. 1971; Urry 1971). The transmembrane motion is performed in several physically distinct steps. In aqueous solution, outside the membrane, the cation carries a hydration shell. Due to strong electrostatic interaction the effective mass of the hydrated ion increases with decreasing ion radius, and thus the effective mobility of the hydrated ion in water increases with increasing ion radius. The diffusion process may be considered as a continuous random walk, i.e. as Brownian motion of the hydrated cation. Upon entering the interior of a channel-like molecule, some of the water molecules have to be stripped off the ion for steric and energetic reasons. For this process it seems to be very important that the channel can respond to the presence of the ion. If the interior is lined with flexible ligands carrying permanent dipole moments, the polarization effect of the ion with respect to the former is the same as with respect to accompanying water molecules. In such pores the reorienting ligands may replace some of the water molecules of the former hydration shell and thus significantly lower the effective dehydration energy. On the other hand an appropriate equilibrium orientation and additional polarization of the ligands lowers the energy barrier imposed on the self-energy of the penetrating ion by the presence of the membrane (Schröder 1984). Due to the more or less regular spacing between ligands in the channel interior the potential profile is given by a sequence of binding sites and barriers, giving rise to a discrete random walk of the ion or another migrating particle (Schröder 1983a).

This well balanced system consisting of aqueous solution, membrane, and molecular channel not only allows for a relatively easy passage of ions including water, but can also show an extremely sensitive ion-specific selectivity, where effective transport rates may differ by orders of magnitude for different ion species. In a previous publication the diffusive process in the form of a one-dimensional random walk for a given set of barriers and binding sites has been discussed and found to be appropriate for well-defined activation energies (Schröder 1983a). A more realistic approach deals with flexible ligands and has the ion's motion restricted to the channel axis (Schröder 1983b). This investigation shows that the mass relevant for the jump process is the effective mass of the ion, which is composed of the ion mass plus the masses of all constituent ligands with their relative weight depending on the distortion field. Thus the actual particle to be considered is the "dressed" ion, the classical counterpart of the small polaron, which means that the mutual coupling

between ion and ligand motion is essential for the transport process. But because of the restricted ion motion the model turns out to be too limited; due to the simple nature of the Coulomb interaction, the transport process is in this case independent of the ion's size, a quantity which is certainly relevant for the selectivity process. In order to obtain a more realistic description, one has to allow for a three-dimensional motion of the ion within the channel. This has been done recently for the simple case of a channel with rigid ligands (Schröder 1985). There it was found that the competing effects of ion size and mass lead to an inversion of the selectivity sequence which would be obtained from the mass dependence alone. For each binding site within the channel the selectivity follows the Eisenman sequence I (Eisenman 1967).

It is the aim of the present work to investigate the influence of flexible ligands on the transport process for ions which can be distinguished by both size and mass, and which can move about arbitrarily inside the channel. It is clear that selectivity sequences observed for different channels are to be taken as effective sequences, i.e. they arise from both intrinsic channel properties and environmental properties. Since the present calculations only yield transport rates due to channel specific properties, conclusions concerning the corresponding effective rates must be drawn with care. Possible implications will be discussed in the last section of this article.

The theoretical discussion of transport properties in systems of interacting particles requires a model of the mutual interaction itself, which is usually static in nature, and a model-independent transport theory, which is kinetic. As long as migration between neighbouring, well defined binding sites is considered, a rate theoretical approach seems to be adequate to describe the basic transport mechanism (Woodbury 1971; Läuger 1973, 1979; Levitt 1978a, 1978b; Hille 1975; Eisenman et al. 1978; Eisenman and Sandblom 1983). However, in all cases, the motion of the ion was assumed to be effectively one-dimensional both in real and phase space. Recently a rate theory allowing for one-dimensional motion in real space and multi-dimensional motion in phase space was introduced (Schröder, unpublished). In the present case the motion of the ion is three-dimensional in real space and multi-dimensional in phase space, which is in principle not different from the one in the previous case. Both situations require the calculation of escape rates across multi-dimensional barriers, where the topology of the hyper-surface created by the many-particle potential follows the motion of the ion. This situation is typical for all systems in which a meta-stable many-particle configuration performs a transition into a different configuration either by emission or absorption of one of the constituent particles. In Sect. I the corresponding generalized rate theoretical formulation is introduced. It allows an application to all problems in which the many-particle potential implies a rate theoretical approach. In Sect. II the interaction model is presented and discussed. The numerical evaluation and discussion of escape rates in relation to molecular parameters follows in the last section.

I. Generalized transition state method for multi-dimensional barriers

Consider a many-particle system consisting of n degrees of freedom denoted by the vector $\boldsymbol{x} = \{x_\mu\}$, $(\mu = 1, \ldots, n)$. The mutual interaction of all particles is supposed to be described by the potential $V(\boldsymbol{x})$ which, for example, may be represented by a sum of pair-potentials or any form of a conservative many-body interaction. Among all possible systems we are interested in the subset of systems which in addition possesses distinct equilibrium states. These states can be identified by local minima on the hyper-surface of the multi-dimensional potential, $V(\boldsymbol{x})$. If the system is thermally activated, i.e. subjected to a heat bath, it may perform transitions from one local minimum to the next one. The basic conception of the transition state method requires the assumption that a configuration, which initially dwells near a minimum eventually reaches a saddle point by thermal activation and from there passes to the next minimum (Kramers 1940). The mean reaction path follows the valley connecting two local minima along the hyper-surface of $V(\boldsymbol{x})$, and the general coordinate-free expression for the rate, Γ, is obtained from the total unidirectional flux across the saddle point (Vineyard 1957).

$$\Gamma = \int \varrho(\dot{\boldsymbol{x}}, \boldsymbol{x})\, (\dot{\boldsymbol{x}}\, \mathrm{d}\boldsymbol{S})\, d^n \dot{x}\,, \quad \dot{\boldsymbol{x}}\, \mathrm{d}\boldsymbol{S} > 0\,. \tag{I.1}$$

Here $\varrho(\dot{\boldsymbol{x}}, \boldsymbol{x})$ is the Boltzmann distribution function and $\mathrm{d}\boldsymbol{S}$ is a hyper-surface element of dimensionality $n-1$, $|\mathrm{d}\boldsymbol{S}| = d^{n-1}x$, cutting through the saddle point. The condition $\dot{\boldsymbol{x}}\, \mathrm{d}\boldsymbol{S} > 0$ guarantees that all contributions to the flux through $\mathrm{d}\boldsymbol{S}$ in forward direction are counted. As long as a transition is possible it can be defined with respect to one degree of freedom, e.g. x_n. If the system is initially near a local equilibrium, a variation of x_n will cause a deviation from this state involving all other degrees of freedom. The direction in which the system moves in n-dimensional configuration-space is then given by the tangent vector

$$\frac{\mathrm{d}\boldsymbol{r}}{\mathrm{d}s_0} = \left\{ \frac{\hat{x}_\mu(x_n)}{\mathrm{d}s_0}, \frac{\mathrm{d}x_n}{\mathrm{d}s_0} \right\}, \quad \mu = 1, \ldots, n-1 \tag{I.2}$$

of the probability current, where ds_0 is the arc length to be associated with the motion of the system in phase space. Thus the rate with respect to x_n can be calculated from the projection of the probability current $\boldsymbol{j}(\boldsymbol{x})$ onto the reaction coordinate x_n. With

$$\Gamma_n = \int \boldsymbol{j}(\boldsymbol{x})\, d\boldsymbol{S} = \int j_0(\boldsymbol{x}) \frac{d\boldsymbol{r}}{ds_0} d\boldsymbol{S} \tag{I.3}$$

and

$$j_0(\boldsymbol{x}) = \int \varrho(\dot{\boldsymbol{x}}, \boldsymbol{x})\, \dot{x}_n\, d^n\dot{x}\,, \quad \dot{x}_n > 0 \tag{I.4}$$

the rate is given by

$$\Gamma_n = \frac{dx_n}{ds_0} \int \varrho(\dot{\boldsymbol{x}}, \boldsymbol{x})\, \dot{x}_n\, d^n\dot{x}\, d^{n-1}x\,, \quad \dot{x}_n > 0\,. \tag{I.5}$$

Thus Γ_n is known if the arc length ds_0 is known. Bearing in mind that the system at any given value of x_n represents an equilibrium configuration with respect to the other $n-1$ degrees of freedom, $\frac{dx_n}{ds_0}$ is readily obtained. The total energy of the system subjected to the heat bath is:

$$E(\dot{\boldsymbol{x}}, \boldsymbol{x}) = \frac{1}{2}\sum_{\mu=1}^{n} m_\mu \dot{x}_\mu^2 + V(\boldsymbol{x})\,. \tag{I.6}$$

Then the desired equilibrium configuration is obtained from a set of $n-1$ equations

$$\frac{\partial V(\boldsymbol{x})}{\partial x_\mu} = f_\mu(\hat{\boldsymbol{x}}(x_n), x_n) = 0\,, \tag{I.7}$$

where $\hat{\boldsymbol{x}}(x_n) = \{\hat{x}_\mu(x_n)\}$, $(\mu = 1, \ldots, n-1)$ denotes the equilibrium positions depending on the selected x_n. Switching to new coordinates $\boldsymbol{q} = \{q_\mu\}$ defined by

$$x_\mu = \hat{x}_\mu(q_n) + q_\mu\,, \quad x_n = q_n \tag{I.8}$$

which refer to possible deviations from the equilibrium values determined by Eq. (I.7), the energy can be written as:

$$E(\dot{\boldsymbol{q}}, \boldsymbol{q}) = \frac{1}{2} m_n \dot{q}_n^2 + \frac{1}{2}\sum_{\mu=1}^{n-1} m_\mu \left(\frac{\partial \hat{x}_\mu}{\partial q_n}\dot{q}_n + \dot{q}_\mu\right)^2 + V(\boldsymbol{q})\,. \tag{I.9}$$

The determination of the saddle point configuration requires:

$$q_\mu = 0\,, \quad (\mu = 1, \ldots, n-1)\,,$$
$$\dot{q}_\mu = 0\,, \quad (\mu = 1, \ldots, n-1)\,.$$

The corresponding energy is:

$$\hat{E} = \frac{1}{2} m_n \left\{1 + \sum_{\mu=1}^{n-1} \frac{m_\mu}{m_n}\left(\frac{\partial \hat{x}_\mu}{\partial q_n}\right)^2\right\} \dot{q}_n^2 + \hat{V}(q_n)\,. \tag{I.10}$$

The kinetic energy can be written as:

$$E_{\mathrm{kin}} = \tfrac{1}{2} m_n \dot{s}_0^2\,.$$

From $\dot{s}_0 = \frac{ds_0}{dq_n}\frac{dq_n}{dt}$ we have:

$$\frac{dq_n}{ds_0} = \frac{1}{\sqrt{1 + \sum_{\mu=1}^{n-1} \frac{m_\mu}{m_n}\left(\frac{\partial \hat{x}_\mu}{\partial q_n}\right)^2}}\,. \tag{I.11}$$

Hence we find for the rate Γ_n:

$$\Gamma_n = \frac{1}{\sqrt{1 + \sum_{\mu=1}^{n-1} \frac{m_\mu}{m_n}\left(\frac{\partial \hat{x}_\mu}{\partial q_n}\right)^2}} \int \varrho(\dot{\boldsymbol{q}}, \boldsymbol{q})\, \dot{q}_n\, d^{n-1}q_n\, d^n\dot{q}\,, \quad \dot{q}_n > 0\,. \tag{I.12}$$

The normalized distribution function is given by:

$$\varrho(\dot{\boldsymbol{q}}, \boldsymbol{q}) = \frac{e^{-\beta E(\boldsymbol{q}, \boldsymbol{q})}}{\int e^{-\beta E(\boldsymbol{q}, \boldsymbol{q})} d^n\dot{q}\, d^n q}\,, \quad \beta = \frac{1}{k_B T}\,. \tag{I.13}$$

The integration over the velocities, $\dot{q}_\mu$, can be carried out by factorizing the integrand, and yields:

$$\frac{\int e^{-\beta E_{\mathrm{kin}}} \dot{q}_n\, d^n\dot{q}}{\int e^{-\beta E_{\mathrm{kin}}} d^n\dot{q}} = \sqrt{\frac{k_B T}{2\pi m_n}}\,.$$

Thus the resulting expression

$$\Gamma_n = \sqrt{\frac{k_B T}{2\pi m_{\mathrm{eff}}}} \frac{Q(q_n = c)}{\int_a^c Q(q_n)\, dq_n} \tag{I.14}$$

contains the effective mass

$$m_{\mathrm{eff}} = m_n + \sum_{\mu=1}^{n-1} m_\mu \left(\frac{\partial \hat{x}_\mu}{\partial q_n}\right)^2 \tag{I.15}$$

and the configurational integral

$$Q(q_n) = \int e^{-\beta V(\boldsymbol{q})}\, d^{n-1}q\,, \tag{I.16}$$

which is closely related to the potential of the mean force, $V_{\mathrm{eff}}(q_n)$:

$$Q(q_n) = Q_0\, e^{-\beta V_{\mathrm{eff}}(q_n)}\,. \tag{I.17}$$

The normalization constant Q_0 is the configurational integral in the absence of the n-th particle:

$$Q_0 = \lim_{q_n \to \infty} Q(q_n)\,.$$

Combining Eqs. (I.14) and (I.17) we finally obtain:

$$\Gamma_n = \sqrt{\frac{k_B T}{2\pi m_{\mathrm{eff}}}} \frac{e^{-\beta V_{\mathrm{eff}}(c)}}{\int_a^c e^{-\beta V_{\mathrm{eff}}(q_n)}\, dq_n}\,. \tag{I.18}$$

The integration along q_n encloses two neighbouring saddle points located at $q_n = a$ and $q_n = c$.

The structure of the expression for the escape rate, Eq. (I.18), obviously does not depend on the dimensionality of the problem. Whereas for a one-particle system its mass and the given potential appear, these quantities are automatically replaced by both effective mass and potential of the many-particle system. In general the diffusing particle

behaves as a dressed particle which depends on all other masses and the mutual interaction via the distortion field $\left\{\frac{\partial \hat{x}_\mu}{\partial q_n}\right\}$. The result of Eq. (I.18) is completely identical with the one found previously in connection with the earlier channel model (Schröder 1983c). It seems remarkable that the present result could have been obtained directly from an effective one-particle energy, namely:

$$\Gamma_n = \frac{\int_0^\infty \dot{q}_n \, \mathrm{d}\dot{q}_n \, \mathrm{e}^{-\beta E_{\mathrm{eff}}(q_n, c)}}{\int_{-\infty}^{\infty} \mathrm{d}\dot{q}_n \int_a^c \mathrm{d}q_n \, \mathrm{e}^{-\beta E_{\mathrm{eff}}(q_n, q_n)}} \tag{I.19}$$

and

$$E_{\mathrm{eff}}(\dot{q}_n, q_n) = \tfrac{1}{2} m_{\mathrm{eff}} \dot{q}_n^2 + V_{\mathrm{eff}}(q_n) \,. \tag{I.20}$$

In its present form, Γ_n holds for all temperatures as well as for arbitrary deviations of the q_μ from zero, in contrast to the harmonic approximations used elsewhere (Vineyard 1957; Weidenmüller and Zhang 1984). Although there is no need to restrict the application of rate theory to the low temperature limit, we will discuss this approximation briefly because of its familiar form.

Let $V_{\mathrm{eff}}(b)$ be the minimum between two enclosing maxima $V_{\mathrm{eff}}(a)$ and $V_{\mathrm{eff}}(c)$. Then the low temperature approximation of Eq. (I.18) is given in the form of the famous Arrhenius law:

$$\Gamma_n \approx \frac{1}{2\pi} \sqrt{\frac{\varkappa(T)}{m_{\mathrm{eff}}}} \, \mathrm{e}^{-\beta \Delta E_{\mathrm{eff}}}, \quad \Delta E_{\mathrm{eff}} \gg k_B T, \tag{I.21}$$

$$\varkappa(T) = \left.\frac{\mathrm{d}^2 V_{\mathrm{eff}}(q_n)}{\mathrm{d}q_n^2}\right|_{q_n = b}, \quad \Delta E_{\mathrm{eff}} = V_{\mathrm{eff}}(c) - V_{\mathrm{eff}}(b) \,.$$

Note that $\varkappa(T)$ is temperature-dependent due to possible anharmonic contributions of the q_μ, and that ΔE_{eff} is a free energy with the entropy of activation

$$\Delta S = k_B \frac{\partial}{\partial T} \left\{ T \ln \frac{Q(c)}{Q(b)} \right\} . \tag{I.22}$$

The very concept of rate theory is reflected in Eqs. (I.18) and (I.21) with the use of the equilibrium distribution function of Eq. (I.13). It has been assumed that an equilibrium configuration of all other degrees of freedom can be ascribed to each value of the reaction coordinate, q_n. Nevertheless, fluctuations around equilibrium appear and are actually time-dependent. They are taken into account by averaging over the subspace perpendicular to q_n, Eq. (I.16). At any given instant the contour of the potential hyper-surface may look very different from the equilibrium contour. Consequently the mean reaction path is the average of all possible and actually performed passages from one minimum to the next, where any deviation from the mean can contribute to the entropy, Eq. (I.22). However, whereas it is true that an equilibrium configuration is assumed by the system for any given value of q_n, it is generally not true that this happens instantaneously following a change of q_n. It is a well known deficiency of the transition state method that it ignores the history of the system prior to a possible transition. But memory effects can become important if the time needed for an adjustment of the system is compatible with the dwelling time in a local minimum or is large compared to it. This is the case if the characteristic frequencies associated with the conformational changes of the system are not large compared to the frequency in the well. For a given set of elastic constants

$$\varkappa_\mu = \left.\frac{\partial^2 V(\boldsymbol{q})}{\partial q_\mu^2}\right|_{q_\mu = 0}$$

the frequencies decrease with increasing masses m_μ. Therefore it cannot be expected that Eqs. (I.18) and (I.21) describe the transition correctly if the m_μ become too large. As it has been shown before, the correction of the rate due to the effective mass may nevertheless become considerable for significantly differing masses within the range of its validity (Schröder et al. 1983).

II. The channel model

The present model combines all properties of the previously used ones (Schröder 1984, 1983c, 1985). The Coulomb interaction with an ion is determined by a helical arrangement of flexible, permanent dipoles which are pointing towards the channel axis with their negative ends. Such flexible ligands, in the form of peptide carbonyl groups are present in the interior of a gramicidin A channel. The helix is assumed to be periodic with constant pitch, $P = 6$ Å, over a total length of 30 Å, carrying 6 dipoles of pairwise alternating orientation per turn. The Coulomb interaction of all ion-dipoles pairs for an ion at arbitrary position $\vec{r}$, is given by

$$U_c = -q \sum_{\mu=1}^{30} \frac{\vec{p}_\mu (\vec{r} - \vec{r}_\mu)}{|\vec{r} - \vec{r}_\mu|^3} , \tag{II.1}$$

where q is the ionic charge and $\vec{p}_\mu$ the dipole moment with $p = |\vec{p}_\mu| = q' d$, where $q' = 0.4\,e$ is its effective charge and $d = 1.24$ Å, its length. The dipoles themselves can perform a hindered rotation in a plane spanned by the radius, $R = 3$ Å, and the axis of the helix. For further evaluation it is convenient to write the Coulomb term in the following form:

$$U_c = -q \sum_{\mu=1}^{30} \frac{(z - z_0\,\mu)\, p_{\parallel \mu} + (\vec{\varrho} - \vec{\varrho}_\mu)\, \vec{p}_{\perp \mu}}{|\vec{r} - \vec{r}_\mu|^3} . \tag{II.2}$$

Here we have introduced the lattice constant $z_0 = 1$ Å.

Also: $|\vec{\varrho}_\mu| = R$, $p_{\parallel\mu} = p \cos \vartheta_\mu$

and $|\vec{p}_{\perp\mu}| = p \sin \vartheta_\mu$.

Since all $\vec{p}_\mu$ are pointing towards the z-axis, one may use the linear-dependence between $\vec{p}_{\perp\mu}$ and $\vec{\varrho}_\mu$:

$$\vec{p}_{\perp\mu} = \lambda \vec{\varrho}_\mu, \quad \lambda = \frac{p}{R} \sin \vartheta_\mu .$$

Thus one obtains:

$$U_c = -p q \sum_{\mu=1}^{30} \frac{(z - z_0 \mu) \cos \vartheta_\mu + R (\vec{\varrho}\, \vec{\varrho}_\mu / R^2 - 1) \sin \vartheta_\mu}{\sqrt{(z - z_0 \mu)^2 + (\vec{\varrho} - \vec{\varrho}_\mu)^2}^3} \tag{II.3}$$

Because the purpose of the present investigation is to study the ion size controlled selectivity effects of a given channel configuration, we neglect the head-to-head binding effect of the dimer (Pullman and Etchebest 1983; Etchebest and Pullman 1984; Etchebest et al. 1984).

The self-energy of the empty channel is given by the elastic but anharmonic restoring forces acting upon each individual dipole:

$$V_{\text{rest}} = -\varepsilon_0 p \sum_{\mu=1}^{30} \{\cos (\vartheta_\mu - \Theta_\mu) - 1\} . \tag{II.4}$$

The polar angles, Θ_μ, represent the undistorted equilibrium orientation of the dipoles with respect to the channel axis, whereas ε_0 is the elastic coupling constant, being equal for all dipoles. The corresponding harmonic potential for small deviations from Θ_μ would be given by

$$V_{\text{rest}} \approx \tfrac{1}{2} \varepsilon_0 p \sum_\mu (\vartheta_\mu - \Theta_\mu)^2 .$$

However, in the present case all calculations will be carried out with the full anharmonic expression, Eq. (II.4), describing hindered rotation. This procedure guarantees a bounded displacement

$$-\pi \leqq \vartheta_\mu - \Theta_\mu \leqq \pi$$

and a correct treatment of the actually temperature-dependent effective potential.

The third contribution to the total interaction in this model is its repulsive part. In contrast to the Coulombic part the much more complex repulsive interaction occurs between the ion and all constituent parts of the molecular channel. Thus it seems to be a fairly good approximation to assume an effective "smeared out" potential of the form

$$V_{\text{rep}} = \tfrac{1}{2} \varkappa_0 \varrho^2 , \tag{II.5}$$

which is actually the harmonic approximation of the complete repulsive term. Thus V_{rep} represents the rest of the non-Coulombic interaction and incorporates ionic as well as molecular properties. We shall revert to this point later.

So far the total interaction is the sum of Eqs. (II.3) – (II.5):

$$V(\vec{r}, \{\vartheta_\mu\}) = -p q \sum_{\mu=1}^{30} \frac{(z - z_0 \mu) \cos \vartheta_\mu + R (\vec{\varrho}\, \vec{\varrho}_\mu / R^2 - 1) \sin \vartheta_\mu}{\sqrt{(z - z_0 \mu)^2 + (\vec{\varrho} - \vec{\varrho}_0)^2}^3} - \varepsilon_0 p \sum_{\mu=1}^{30} \{\cos (\vartheta_\mu - \Theta_\mu) - 1\} + \tfrac{1}{2} \varkappa_0 \varrho^2 . \tag{II.6}$$

According to Eq. (I.6) the total energy is

$$E = \tfrac{1}{2} d^2 \sum_{\mu=1}^{30} m_\mu \dot{\vartheta}_\mu^2 + \tfrac{1}{2} m_0 \dot{\vec{r}}^2 + V(\vec{r}, \{\vartheta_\mu\}) , \tag{II.7}$$

where m_0 is the mass of the ion. Altogether this system possesses 33 degrees of freedom, where 3 of them belong to the ion. The transport quantity of interest is the jump rate from well to well along the channel. Thus the reaction coordinate to be selected is the z-axis. Therefore, the remaining 32 variables are subject to a linear transformation according to Eq. (I.8). For this purpose it is convenient to start with the angular variables ϑ_μ, for which we write:

$$\vartheta_\mu = \hat{\vartheta}_\mu + \alpha_\mu . \tag{II.8}$$

Here $\hat{\vartheta}_\mu = \hat{\vartheta}_\mu (\vec{r})$ is the equilibrium orientation of the μ-th dipole following the position of the ion. α_μ is the spontaneous deviation independent of $\vec{r}$. The set of 30 $\hat{\vartheta}_\mu$ is obtained from the set of 30 conditions

$$\frac{\partial V(\vec{r}, \{\vartheta_\mu\})}{\partial \vartheta_\mu} = 0 ! \tag{II.9}$$

The use of the formulation

$$V(\vec{r}, \{\vartheta_\mu\}) = -\sum_{\mu=1}^{30} \{A_\mu (\vec{r}) \cdot \cos \vartheta_\mu + B_\mu (\vec{r}) \cdot \sin \vartheta_\mu - \varepsilon_0 p\} + \tfrac{1}{2} \varkappa_0 \varrho^2$$

yields the equilibrium orientations as:

$$\cos \hat{\vartheta}_\mu = \frac{A_\mu (\vec{r})}{\sqrt{A_\mu (\vec{r})^2 + B_\mu (\vec{r})^2}} . \tag{II.10}$$

The change of variables to the set $\{\alpha_\mu\}$ simplifies the expression for the potential energy:

$$V(\vec{r}, \{\alpha_\mu\}) = -\sum_{\mu=1}^{30} [W_\mu (\vec{r}) \cos \alpha_\mu - \varepsilon_0 p] + \tfrac{1}{2} \varkappa_0 \varrho^2 . \tag{II.11}$$

The summation coefficients used are:

$$W_\mu (\vec{r}) = \sqrt{A_\mu (\vec{r})^2 + B_\mu (\vec{r})^2} ,$$

$$A_\mu (\vec{r}) = \frac{p q (z - z_0 \mu)}{\sqrt{(z - z_0 \mu)^2 + (\vec{\varrho} - \vec{\varrho}_\mu)^2}^3} + \varepsilon_0 p \cos \Theta_\mu ,$$

$$B_\mu (\vec{r}) = \frac{p q R (\vec{\varrho}\, \vec{\varrho}_\mu / R^2 - 1)}{\sqrt{(z - z_0 \mu)^2 + (\vec{\varrho} - \vec{\varrho}_\mu)^2}^3} + \varepsilon_0 p \sin \Theta_\mu .$$

In the form of Eq. (II.11) the potential is described correctly for any position of the ion. However, the ion's motion is restricted to the interior of the channel, so that $|\vec{\varrho}| < R$ holds generally.

In our interaction model such a confinement of an ion can always be guaranteed by the choice of a sufficiently large parameter, $\varkappa_0$. In the limit $\varkappa_0 \to \infty$ the motion is restricted to the channel axis, thus a finite value of $\varkappa_0$ is associated with a finite deviation $\vec{\varrho}_0$ off the z-axis. At any given position along the z-axis an equilibrium position $\vec{\varrho}_0(z)$ can be found, where the Coulomb forces just cancel the repulsive forces. Considering a finite ion radius as well as a spatial extension of the ligands, $|\vec{\varrho}_0(z)|$ must be considerably smaller than R. With this condition an expansion of $V(\vec{\varrho}, z, \{\alpha_\mu\})$ around $\vec{\varrho}=0$ is justified. Since the repulsive part is already given as a harmonic expansion, it is only necessary to expand the Coulomb term up to second-order in $\vec{\varrho}$, thereby avoiding third and higher-order cross-terms in $\vec{\varrho}$ and α_μ. In order to retain the full anharmonic dependence on the α_μ, we use the identity

$$W_\mu(\vec{r}) \cos\alpha_\mu = W_\mu(\vec{\varrho}, z)\,(\cos\alpha_\mu - 1) + W_\mu(\vec{\varrho}, z)\,.$$

The first term on the RHS starts with α_μ^2. Therefore any expansion term other than $W_\mu(0,z)$ would lead to a higher than second-order contribution in $\vec{\varrho}$ and α_μ. The second term is expanded up to terms in $\vec{\varrho}^2$, leading to the following approximation:

$$W_\mu(\vec{r}) \cos\alpha_\mu \approx W_\mu(0,z)\cos\alpha_\mu + \vec{\varrho}\,\frac{\partial}{\partial\vec{\varrho}}\,W_\mu(\vec{\varrho},z)\Big|_{\vec{\varrho}=0} + \frac{1}{2}\left(\vec{\varrho}\,\frac{\partial}{\partial\vec{\varrho}}\right)^2 W_\mu(\vec{\varrho},z)\Big|_{\vec{\varrho}=0}\,. \qquad \text{(II.12)}$$

It should be noted that in this approximation the equilibrium orientations $\hat{\vartheta}_\mu$ are not taken for $\vec{\varrho}=0$. In contrast, Eq. (II.12) implies an expansion of the $\hat{\vartheta}_\mu$ up to second order in $\vec{\varrho}$. With the substitution of Eq. (II.12) into Eq. (II.11) and a rearrangement of terms we obtain

$$V(\vec{r}, \{\alpha_\mu\}) = -\sum_{\mu=1}^{30} [W_\mu(z)\cos\alpha_\mu - \varepsilon_0 p] + \vec{A}(z)\,\vec{\varrho} + \tfrac{1}{2}\,\vec{\varrho}\,\vec{\vec{B}}(z)\,\vec{\varrho} \qquad \text{(II.13)}$$

with

$$\vec{A}(z) = -\sum_{\mu=1}^{30} \frac{\partial W_\mu(\vec{r})}{\partial\vec{\varrho}}\Big|_{\vec{\varrho}=0}$$

and:

$$\vec{\vec{B}}(z) = 1\cdot\varkappa_0 - \frac{\partial}{\partial\vec{\varrho}} * \frac{\partial}{\partial\vec{\varrho}} \sum_{\mu=1}^{30} W_\mu(\vec{r})\Big|_{\vec{\varrho}=0}\,.$$

The equilibrium position $\vec{\varrho}_0(z)$ follows from

$$\frac{\partial V(z,\vec{\varrho},\{\alpha_\mu\})}{\partial\vec{\varrho}} = 0\,.$$

Hence:

$$\vec{\varrho}_0(z) = -\vec{\vec{B}}(z)^{-1}\cdot\vec{A}(z)\,. \qquad \text{(II.14)}$$

The stability of the equilibrium position is guaranteed by the simultaneous conditions

$$B_{11} > 0 \quad \text{and} \quad B_{11}B_{22} - B_{12}^2 > 0 \qquad \text{(II.15)}$$

for the dyadic

$$\vec{\vec{B}} = \begin{pmatrix} B_{11} & B_{12} \\ B_{12} & B_{22} \end{pmatrix}.$$

In analogy to Eq. (II.8), $\vec{\varrho}$ is split into $\vec{\varrho}_0(z)$ and the deviation from equilibrium $\delta\vec{\varrho}$:

$$\vec{\varrho} = \vec{\varrho}_0(z) + \delta\vec{\varrho}\,. \qquad \text{(II.16)}$$

With the use of Eq. (II.14) we finally obtain the desired form of the potential corresponding to $V(\boldsymbol{q})$ in Eq. (I.9):

$$V(z,\delta\vec{\varrho},\{\alpha_\mu\}) = -\sum_{\mu=1}^{30}[W_\mu(z)\cos\alpha_\mu - \varepsilon_0 p] - \tfrac{1}{2}\vec{A}\,\vec{\vec{B}}^{-1}\vec{A} + \tfrac{1}{2}\,\delta\vec{\varrho}\,\vec{\vec{B}}\,\delta\vec{\varrho}\,. \qquad \text{(II.17)}$$

In the next step the kinetic energy must be expressed in the same new variables. For this purpose we start again with the angular variables:

$$E_{\text{kin}} = \tfrac{1}{2}\,\mathrm{d}^2 \sum_{\mu=1}^{30} m_0\,(\nabla\hat{\vartheta}_\mu\,\dot{\vec{r}} + \dot{\alpha}_\mu)^2 + \tfrac{1}{2}\,m_0\,\dot{\vec{r}}^2\,. \qquad \text{(II.18)}$$

Here we must consider a correction of the equilibrium orientation, $\hat{\vartheta}_\mu$, due to a deviation of the ion from the z-axis. Using the linear response approximation, i.e. carrying only first-order derivatives, namely

$$\hat{\vartheta}_\mu(\vec{r}) \approx \hat{\vartheta}_\mu(0,z) + \vec{\varrho}\,\frac{\partial}{\partial\vec{\varrho}}\,\hat{\vartheta}_\mu(\vec{\varrho},z)\Big|_{\vec{\varrho}=0}$$

we obtain for the kinetic energy:

$$E_{\text{kin}} = \frac{1}{2}\,\mathrm{d}^2 \sum_{\mu=1}^{30} m_0 \left\{\left(\frac{\partial\hat{\vartheta}_\mu}{\partial\vec{\varrho}}\right)_{\vec{\varrho}=0}\dot{\vec{\varrho}} + \left(\frac{\partial\hat{\vartheta}_\mu}{\partial z}\right)_{\vec{\varrho}=0}\dot{z} + \dot{\alpha}_\mu\right\}^2 + \frac{1}{2}\,m_0\,(\dot{\vec{\varrho}}^2 + \dot{z}^2)\,. \qquad \text{(II.19)}$$

In addition we have to introduce

$$\dot{\vec{\varrho}} = \frac{\partial\vec{\varrho}_0}{\partial z}\,\dot{z} + \delta\dot{\vec{\varrho}}\,,$$

where $\vec{\varrho}_0$ follows from Eq. (II.14).
Hence:

$$E_{\text{kin}} = \frac{1}{2}\,\mathrm{d}^2 \sum_{\mu=1}^{30} m_\mu \left\{\left[\left(\frac{\partial\hat{\vartheta}_\mu}{\partial\vec{\varrho}}\right)_{\vec{\varrho}=0}\frac{\partial\vec{\varrho}_0}{\partial z} + \left(\frac{\partial\hat{\vartheta}_\mu}{\partial z}\right)_{\vec{\varrho}=0}\right]\dot{z} + \left(\frac{\partial\hat{\vartheta}_\mu}{\partial\vec{\varrho}}\right)_{\vec{\varrho}=0}\delta\dot{\vec{\varrho}} + \dot{\alpha}_\mu\right\}^2 + \frac{1}{2}\,m_0\left\{\left(\frac{\partial\vec{\varrho}_0}{\partial z}\,\dot{z} + \delta\dot{\vec{\varrho}}\right)^2 + \dot{z}^2\right\}. \qquad \text{(II.20)}$$

In the final step the effective mass and the potential of the mean force have to be evaluated. The effective mass is obtained directly from the projection of the mean reaction path onto the reaction coordinate z:

$$\sqrt{m_{\text{eff}}} = \sqrt{m_0}\,\frac{\mathrm{d}s_0}{\mathrm{d}z}.$$

The static equilibrium configuration is in any case defined by

$$\alpha_\mu = 0\,,\quad \dot{\alpha}_\mu = 0\,,\quad (\mu = 1, \ldots, 30)$$
$$\delta\vec{\varrho} = 0\,,\quad \delta\dot{\vec{\varrho}} = 0\,.$$

Thus the effective mass is

$$m_{\text{eff}} = \sqrt{m_0\left[1+\left(\frac{\partial\vec{\varrho}_0}{\partial z}\right)^2\right] + \mathrm{d}^2\sum_{\mu=1}^{30} m_\mu\left[\left(\frac{\partial\hat{\vartheta}_\mu}{\partial\vec{\varrho}}\right)_{\vec{\varrho}=0}\cdot\frac{\partial\vec{\varrho}_0}{\partial z}+\left(\frac{\partial\hat{\vartheta}_\mu}{\partial z}\right)_{\vec{\varrho}=0}\right]^2}, \tag{II.21}$$

where z has to be taken at the saddle point. The configurational integral, Eq. (I.16), is for the present potential, Eq. (II.17), given by a product of integrals

$$Q(z) = \int \mathrm{e}^{-\beta V}\,\mathrm{d}^n\chi\cdot\mathrm{d}^2(\delta\vec{\varrho})\,,$$

which can be factorized as follows:

$$Q(z) = \mathrm{e}^{\frac{1}{2}\beta\vec{A}\ddot{\vec{B}}^{-1}\vec{A}}\int \mathrm{e}^{-\frac{1}{2}\beta\delta\vec{\varrho}\ddot{\vec{B}}\delta\vec{\varrho}}\,\mathrm{d}^2(\delta\vec{\varrho}) \cdot\prod_{\mu=1}^{30}\int_{-1}^{+1}\mathrm{d}\chi_\mu\,\mathrm{e}^{\beta[W_\mu\chi_\mu-\varepsilon_0 p]}.$$

Here $\cos\alpha_\mu = \chi_\mu$ has been used. (II.22)

$$Q(z) = \frac{2\pi k_B T}{\sqrt{\det\ddot{\vec{B}}}}\,\mathrm{e}^{\frac{1}{2}\beta\vec{A}\ddot{\vec{B}}^{-1}\vec{A}}\prod_{\mu=1}^{30}\left\{\frac{\mathrm{e}^{-\beta\varepsilon_0 p}\,(\mathrm{e}^{\beta W_\mu}-\mathrm{e}^{-\beta W_\mu})}{\beta W_\mu}\right\}.$$

The configurational integral, Eq. (II.22), in the absence of the ion is simply given by:

$$\lim_{|z|\to\infty} Q(z) = Q_0\,.$$

With $\lim_{|z|\to\infty} W_\mu(z) = \varepsilon_0 p$ follows:

$$Q_0 = \frac{2\pi k_B T}{\varkappa_0}\left\{\frac{\mathrm{e}^{-\beta\varepsilon_0 p}\,(\mathrm{e}^{\beta\varepsilon_0 p}-\mathrm{e}^{-\beta\varepsilon_0 p})}{\beta\varepsilon_0 p}\right\}^{30}. \tag{II.23}$$

Finally we obtain from

$$\frac{Q(z)}{Q_0} = \mathrm{e}^{-\beta V_{\text{eff}}(z)}$$

as the potential of the mean force:

$$V_{\text{eff}}(z) = -k_B T\sum_{\mu=1}^{30}\ln\frac{\sin h(\beta W_\mu)}{\beta W_\mu} + k_B T\sum_{\mu=1}^{30}\ln\frac{\sin h(\beta\varepsilon_0 p)}{\beta\varepsilon_0 p} - \frac{1}{2}\vec{A}\ddot{\vec{B}}^{-1}\vec{A} - k_B T\ln\frac{\varkappa_0}{\sqrt{\det\ddot{\vec{B}}}}. \tag{II.24}$$

The first term on the RHS of Eq. (II.24) is the restricted free energy of the system with the ion moving along the z-axis, whereas the second term is the negative free energy of the empty channel. This term serves to normalize the former, i.e. $\lim_{|z|\to\infty} V_{\text{eff}} = 0$.

The third term represents the temperature-independent correction of the potential due to the actual three-dimensional motion. The fourth term is purely entropic; its presence reflects the fact that the projection of the mean reaction path onto real space, namely the equilibrium path $\{\vec{\varrho}_0(z), z\}$, is the average of all possible trajectories

$$\{\vec{\varrho}_0 + \delta\vec{\varrho}, z\}\,.$$

An analogous argument holds for the entropic part of the first term on the RHS of Eq. (II.24). The potential of the mean force for zero temperature is identical with $V(z, \delta\vec{\varrho}, \{\alpha_\mu\})$ for $\delta\vec{\varrho} = 0$ and all $\alpha_\mu = 0$, i.e. with $\hat{V}$ in Eq. (I.10)

$$\lim_{T\to 0} V_{\text{eff}}(z) = -\sum_{\mu=1}^{30}(W_\mu - \varepsilon_0 p) - \tfrac{1}{2}\vec{A}\ddot{\vec{B}}^{-1}\vec{A}\,. \tag{II.25}$$

In the following section the numerical results for the equilibrium path $\{\vec{\varrho}_0(z), z\}$, the potential $V_{\text{eff}}(z)$ and the rate

$$\Gamma = \sqrt{\frac{k_B T}{2\pi m_{\text{eff}}}}\,\frac{\mathrm{e}^{-\beta V_{\text{eff}}(c)}}{\int_a^c \mathrm{d}z\,\mathrm{e}^{-\beta V_{\text{eff}}(z)}} \tag{II.26}$$

will be discussed in detail.

III. Discussion of numerical results

All quantities of interest, such as the equilibrium path, the potential of the mean force, the escape rates, etc. are the results of elementary calculations. All derivatives can be evaluated analytically and have been fed into an appropriate numerical routine performing the summation over all dipoles and the one remaining numerical integration in the configurational integral, Eq. (II.26). This procedure requires the input of the dipole position-dependent undistorted equilibrium orientations Θ_μ, as introduced in Eq. (II.4). In order to obtain a gramicidin-like structure, orientationally alternating dipoles in the following sequence are used:

$$\Theta_\mu = \vartheta_0\,,\quad \Theta_{\mu+1} = 180° - \vartheta_0\,,$$

where $\vartheta_0 = -20°$ and $\Theta_1 = \vartheta_0$. There are two free molecular parameters ε_0 and $\varkappa_0$, which are replaced by the dimensionless quantities

$$\varepsilon = \frac{\varepsilon_0 z_0^2}{q}, \quad \varkappa = \frac{1}{3}\frac{\varkappa_0 z_0^2}{V_0}$$

with $V_0 = \frac{qp}{z_0^2}$. The position along the z-axis is expressed by $\zeta = z/z_0$. The two variables ε and $\varkappa$ control the flexibility of the ligands and the size of the ion, respectively. For $\varepsilon = 0$ the dipoles are rotating freely, whereas for $\varepsilon \to \infty$ they become rigid. For a given temperature T, ε is representative for the average fluctuations of the individual ligands. Only at $T = 0$ do all α_μ vanish identically. At finite temperatures all even moments $\langle \alpha_\mu^{2n} \rangle$ are different from zero:

$$\langle \cos \alpha_\mu \rangle = \frac{\int \cos \alpha_\mu \, e^{\beta W_\mu \cos \alpha_\mu} \, d(\cos \alpha_\mu)}{\int e^{\beta W_\mu \cos \alpha_\mu} \, d(\cos \alpha_\mu)}.$$

Hence:

$$\langle \cos \alpha_\mu \rangle = \coth(\beta W_\mu) - \frac{1}{\beta W_\mu}. \tag{III.1}$$

If there is no ion in the immediate neighbourhood of a dipole, its mean deviation can be approximated by

$$\langle \cos \alpha_\mu \rangle \approx \coth(\beta V_0 \varepsilon) - \frac{1}{\beta V_0 \varepsilon}. \tag{III.2}$$

Librations of the ligands between 10° and 20° at room temperature are reasonable. Thus the corresponding values of ε with $0.25 \lesssim \varepsilon \lesssim 0.8$ can be considered realistic.

The meaning of $\varkappa$ becomes obvious from Eq. (II.14); it can be seen that $\varkappa$ directly determines the shape of the three-dimensional equilibrium path along the channel. For large $\varkappa$ the deviation off the z-axis becomes proportional to $\varkappa^{-1}$ and shrinks to zero as $\varkappa \to \infty$, i.e. the motion becomes linear. The smaller $\varkappa$ is, the smaller the separation between the ion and the negative end of a dipole can be. This separation is finally only restricted by the ion radius and the spatial extension of the ligands. In the present model the steric contribution of the ion-channel interaction is represented by an effective inner radius, R_{eff}, of the pore and the ion radius, R_I. Since $\varkappa$ is position independent, R_{eff} defines a cylindrical hole with constant radius. For a given ion radius the relation

$$|\vec{\varrho}_{\text{Max}}| = R_{\text{eff}} - R_I \tag{III.3}$$

fixes the maximum possible deviation, $|\vec{\varrho}_{\text{Max}}|$, off the axis. On the other hand $\vec{\varrho}_0(\zeta)$ is finite for any $\varkappa$ as long as the condition of Eq. (II.15) is fulfilled. Therefore the value of $\varkappa$ to be associated with a given ion radius is easily identified with the aid of Eq. (III.3). There is a one-to-one correspondency between $\varkappa$ and the required $|\vec{\varrho}_{\text{Max}}|$ for a given channel. Different channels are to be distinguished by different parameters, ε. Since there is a coupling mechanism between the three-dimensional motion of the ion and the reorientation of the dipoles, it is clear that any value of $\varkappa$ satisfying Eq. (III.3) implicitly depends on ε. Requiring the same maximal distance off the z-axis for the same ion in different channels leads to different values of $\varkappa$. Consequently only one independent parameter, namely ε, remains if ion radii and effective pore radius are considered as constants. For the present model $R_{\text{eff}} = 2$ Å, which again comes close to the pore radius for gramicidin A. Using the Pauling radii for alkali ions the equilibrium path has been calculated for all five ions and for two different channels with $\varepsilon = 0.05$ and $\varepsilon = 0.3$, respectively. The graphic results are shown in Fig. 1a–d for sodium and caesium. For both Na^+ and Cs^+ there is a distinct difference between a "soft" channel with $\varepsilon = 0.05$ and a "hard" channel with $\varepsilon = 0.3$. Whereas the projection of the path onto the molecular $x-y$ plane is almost circular for the former, it shows cusp-line turning points for the latter, especially in the case of Na^+. In all examples the respective $|\vec{\varrho}_{\text{Max}}|$ appears periodically with a three-fold symmetry and can easily be determined. Actually, $|\vec{\varrho}_{\text{Max}}|$ can be represented as a function of $\varkappa$ for a given ε. This has been done explicitly for $\varepsilon = 0.3$ in Fig. 2. Fixing $|\vec{\varrho}_{\text{Max}}|$ by $R_{\text{eff}} - R_I$ one immediately obtains the relevant $\varkappa$. This procedure yields the following list of parameters for the five alkali ions:

	R_I [Å]	$\lvert\vec{\varrho}_{\text{Max}}\rvert$ [Å]	$\varkappa(\varepsilon = 0.05)$	$\varkappa(\varepsilon = 0.3)$
Li^+	0.60	1.40	0.0322	0.0372
Na^+	0.95	1.05	0.0377	0.0419
K^+	1.33	0.67	0.0500	0.0525
Rb^+	1.48	0.52	0.0598	0.0611
Cs^+	1.69	0.31	0.0896	0.0868

According to this list a well defined value of $\varkappa$ depending only on ε can be attributed to each specific ion with a given radius. The method employed here will also be used later to calculate the jump rates for the complete set of alkali ions, depending only on the ligand flexibility. The quantities shown above have been used to evaluate the different channel profiles from Eq. (II.24) as seen by the five different ions. These examples are demonstrated in Fig. 3a+b, where only one half of the symmetric (with respect to ζ) potential is shown.

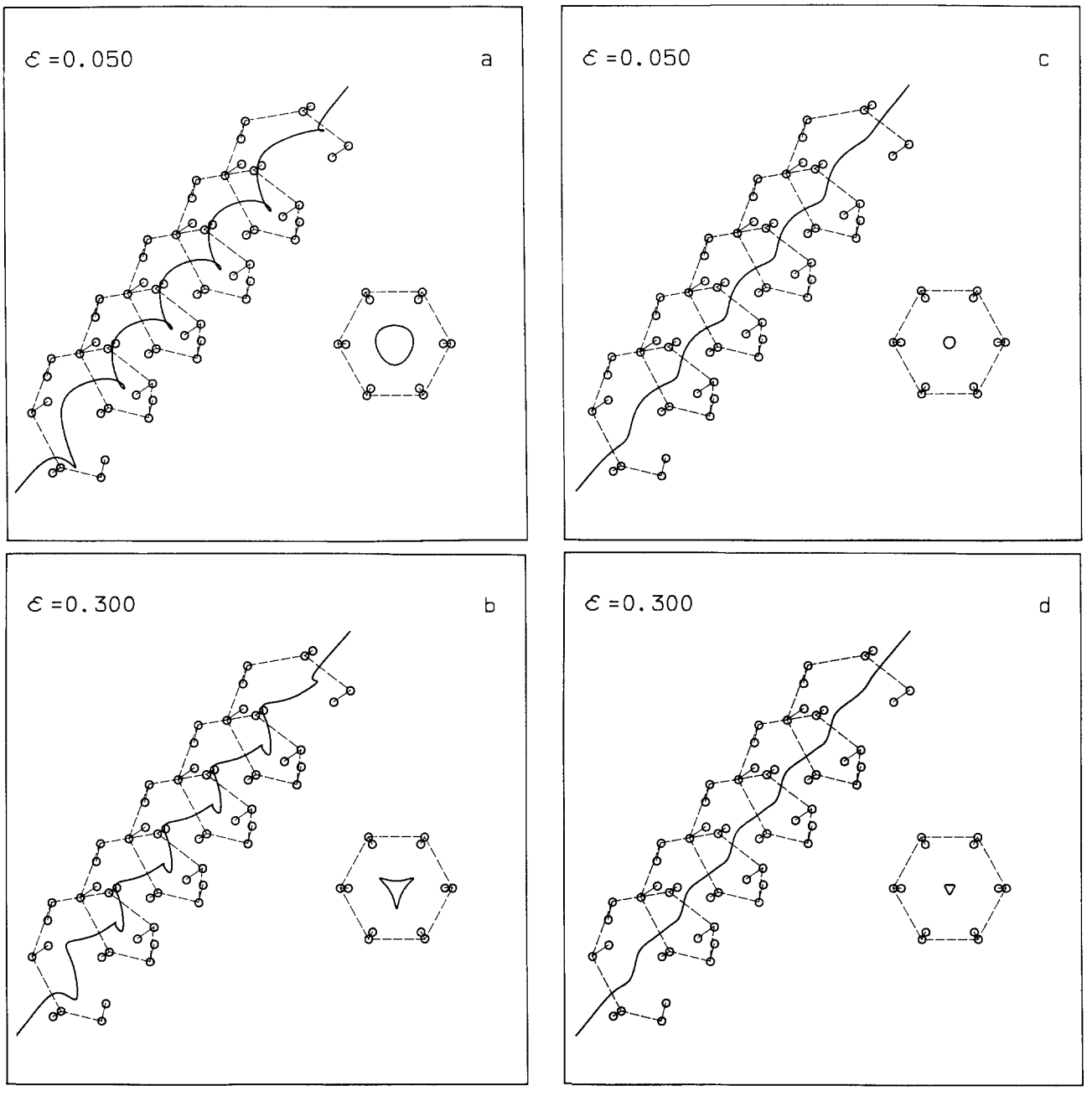

Fig. 1a. The three-dimensional equilibrium path of a Na^+ ion along a "soft" channel ($\varepsilon = 0.05$) and its projection onto the molecular $x-y$ plane. **b** The three-dimensional equilibrium path of a Na^+ ion along a "hard" channel ($\varepsilon = 0.3$) and its projection onto the molecular $x-y$ plane. **c** The three-dimensional equilibrium path of a Cs^+ ion along a "soft" channel ($\varepsilon = 0.05$) and its projection onto the molecular $x-y$ plane. **d** The three-dimensional equilibrium path of a Cs^+ ion along a "hard" channel ($\varepsilon = 0.3$) and its projection onto the molecular $x-y$ plane

For a discussion of the characteristic properties let us recall the expression for the potential:

$$V_{\text{eff}}(\zeta) = -k_B T \sum_{\mu=1}^{30} \ln \frac{\sin h\,(\beta W_\mu)}{\beta W_\mu} + k_B T \ln \left\{ \frac{\sin h\,(\beta V_0 \varepsilon)}{\beta V_0 \varepsilon} \right\}^{30} - \frac{1}{2} \vec{A}\, \overleftrightarrow{B}^{-1} \vec{A} - k_B T \ln \frac{3 \varkappa V_0}{z_0^2 \sqrt{\det \overleftrightarrow{B}}}. \quad \text{(III.4)}$$

It is clear that larger ions, such as Rb^+ and Cs^+, are moving around in the immediate neighbourhood of the channel axis, whereas smaller ions, such as Li^+ and Na^+, can dive into the ligand conformation. The consequence is a generally decreasing activation energy for the individual wells with increasing ion radius and an increasingly flat structure of the whole channel. It is also very instructive to see that some of the maximal 15 binding-sites disappear for the

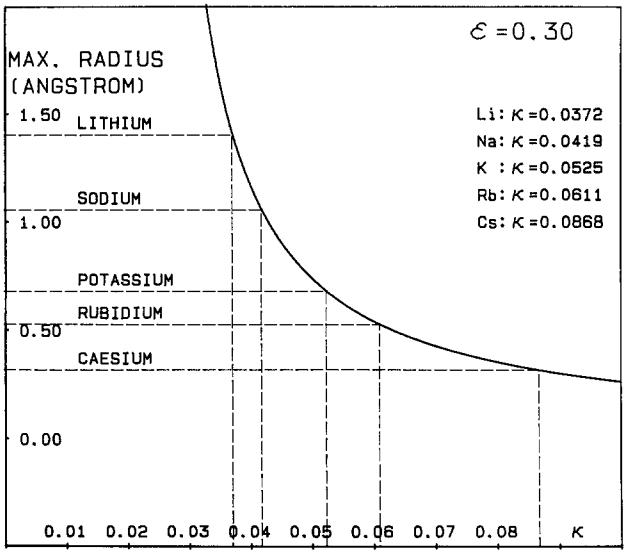

Fig. 2. The maximum possible separation between channel axis and ion centre as a function of the coupling constant $\varkappa$. The values for the five different ions are shown by dashed lines

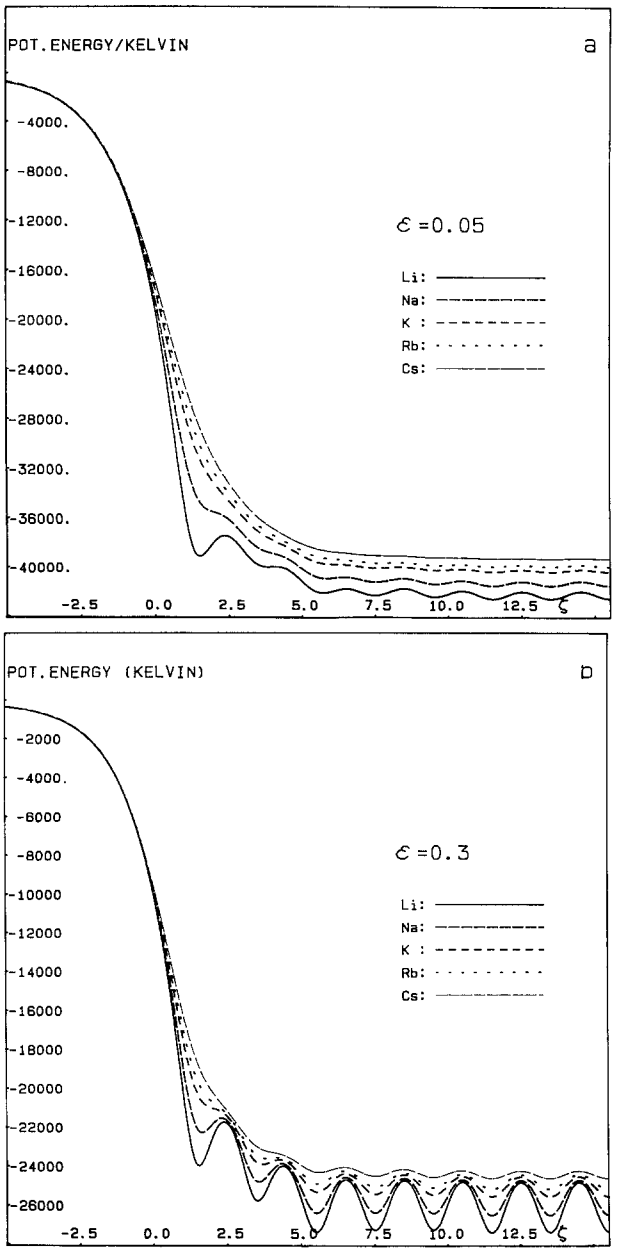

Fig. 3a. The potential profiles due to Coulomb and polarization energies as a function of the respective ion position, ζ, for the five alkali ions in a "soft" channel ($\varepsilon = 0.05$) at $T = 300$ K. **b** The potential profiles due to Coulomb and polarization energies as a function of the respective ion position, ζ, for the five alkali ions in a "hard" channel ($\varepsilon = 0.3$) at $T = 300$ K.

larger ions. This striking result leads to the conclusion that phenomenological channel models with a fixed number of binding sites and barriers are probably not appropriate to correctly interpret experimental findings. The same channel may appear differently to different ions. The third and the fourth terms on the RHS of Eq. (III.4) are responsible for the variation of the potential if the ion can move off the axis. Dominating is the third term, which of all terms gives the largest contribution to the activation energy, whereas the entropic term shows rather small variations. If $\varkappa$ is large enough, both contributions can be neglected, and the only varying term is the first one on the RHS of Eq. (III.4). It describes the potential in the case of the one-dimensional motion along the axis. The profiles for Cs^+ are essentially due to this contribution.

A variation with respect to ε affects the potential in two different ways. Firstly, decreasing ε increases the total binding energy of the whole channel (note the difference in scale between Fig. 3a and b!). Dipoles of high mobility reorientate easily towards an ion with the tendency of charging the channel interior more negatively. Secondly, the individual activation energies increase monotonically with increasing ε until a maximum value is reached asymptotically for $\varepsilon \to \infty$, if $\varkappa$ is large. In the case of small ions the situation is different. For constant $\varkappa$ the activation energy of a single binding site reaches a maximum in the vicinity of $\varepsilon \approx 0.3$ and decreases monotonically for larger values of ε. For constant ε the activation energies are increasing with decreasing $\varkappa$, as can be seen from Fig. 4, which shows the activation energy for the central binding site ($14.5 \leqq \zeta \leqq 10.5$) as a function of ε, at fixed $\varkappa$. The temperature is the same as in Fig. 3a+b, namely $T = 300$ K. The behaviour of ΔE_{eff}, Eq. (I.21), as a function of ε demonstrates convincingly that channels with certain polarizability properties can exhibit a tremendous power of selectivity. In the present case the most pronounced effects are to be expected in the vicinity of $\varepsilon = 0.3$. In this region the

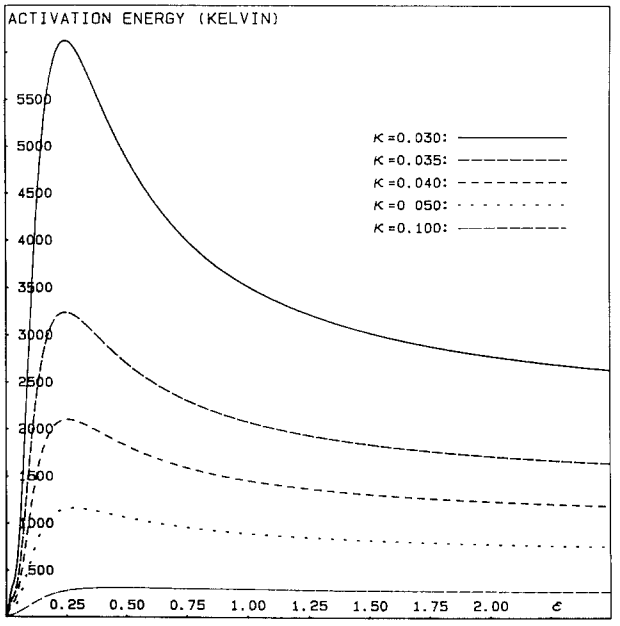

Fig. 4. The activation energies of the central binding site as a function of the ligand flexibility, ε, for different ion sizes (expressed by independently chosen values of $\varkappa$)

increase in ΔE_{eff} with decreasing ion size is most dramatic.

The variation of the escape rates with varying ion radius depends on the actual relation between ε and $\varkappa$, and is therefore model-dependent. Moreover, it depends on ion as well as on ligand masses. In the next step the rates of escape from the central binding site will be calculated using the dependence of $\varkappa$ upon ε established before. The ingredients for the calculation of the escape rate

$$\Gamma = \frac{1}{z_0}\sqrt{\frac{k_B T}{2\pi m_{\text{eff}}}}\,\frac{e^{-\beta V_{\text{eff}}(c)}}{\int_a^c d\zeta\, e^{-\beta V_{\text{eff}}(\zeta)}} \qquad \text{(III.5)}$$

are the potential of the mean force $V_{\text{eff}}(\zeta)$, Eq. (III.4), and the effective mass according to Eq. (II.21). As in previous calculations (Schröder 1983b, c), all ligand masses are assumed to be equal with

$$m_\mu = m_D \triangleq 0.695\ \text{Na}\,.$$

For the central binding site we have $a = 14.5$ and $c = 16.5$, where m_{eff} has to be taken at $\zeta = c$. The temperature is again $T = 300$ K. For the present, $\varkappa$ and ε have been taken as independent parameters, where the rates have been evaluated as a function of $\varkappa$ for two different channels, namely for $\varepsilon = 0.05$ and $\varepsilon = 0.3$. The result is shown in Fig. 5a+b. Along each curve the respective ion mass is a constant. For both the channels, the sequence of the rates follows the sequence of the respective ion masses, i.e. small ions are favoured. However, mass and radius are not independent. Therefore, only one point on each curve belongs to the matching pair of radius R_I and ion mass m_0, where R_I is to be represented by the corresponding $\varkappa$. These points have been marked by crosses and are given by the $\varkappa$ values listed before. Thus a unique relation between ion mass and the interaction parameter $\varkappa$ has been established.

The corresponding rates can easily be read from Fig. 5a+b. The numbers are as follows:

	$\Gamma(\varepsilon=0.05)$	$\Gamma(\varepsilon=0.3)$	$\Gamma(\varepsilon=\infty)$ [s^{-1}]
Li^+	$1.60 \cdot 10^{11}$	$6.21 \cdot 10^{8}$	$2.79 \cdot 10^{9}$
Na^+	$1.98 \cdot 10^{11}$	$4.30 \cdot 10^{9}$	$9.15 \cdot 10^{9}$
K^+	$2.76 \cdot 10^{11}$	$3.81 \cdot 10^{10}$	$4.56 \cdot 10^{10}$
Rb^+	$2.30 \cdot 10^{11}$	$5.98 \cdot 10^{10}$	$6.02 \cdot 10^{10}$
Cs^+	$2.27 \cdot 10^{11}$	$1.22 \cdot 10^{11}$	$1.14 \cdot 10^{11}$

The numbers in the third row are the results of the rigid channel (Schröder 1985), which have been added for comparison. It is evident that in all cases the rates depending on both mass and radius differ greatly from the rates depending on the mass only. Most striking is the influence of the channel polarizability. Whereas the ratio between Cs^+ and Li^+ is about 40 for the rigid channel, it is 200 (!) for the channel with $\varepsilon = 0.3$. It is also obvious that the polarizability of the channel affects smaller ions more strongly than larger ones. Since the separation between ion and ligands depends on the ion radius, the polarization energy increases with decreasing ion radius. Thus the polaron-like character of the ion-ligand system is more pronounced for smaller than for larger ions, and more for "soft" channels than for "hard" ones. With the increase of the activation energy for small ions the mean residence time of the ion at a binding site increases, or in other words, the lifetime of the polaron increases. However, this increase in dwelling time is not only due to the activation energy. In addition, smaller ions travel longer than larger ones, because the distance connecting two points in configuration space shrinks with increasing ion size. For given ion mass the effective mass increases with decreasing $\varkappa$. This effect is evident from Fig. 1a–d.

The aforementioned method employed to associate given ion mass and radius with the model parameter $\varkappa$ is used in the final step of this discussion to present the individual ionic escape rates as continuous functions, $\Gamma(\varepsilon)$, of the elastic constant ε. That means that a rate with respect to any binding site within the channel, and therefore the transmembrane current, can be expressed by a one-parametric function, where the potential profile for different

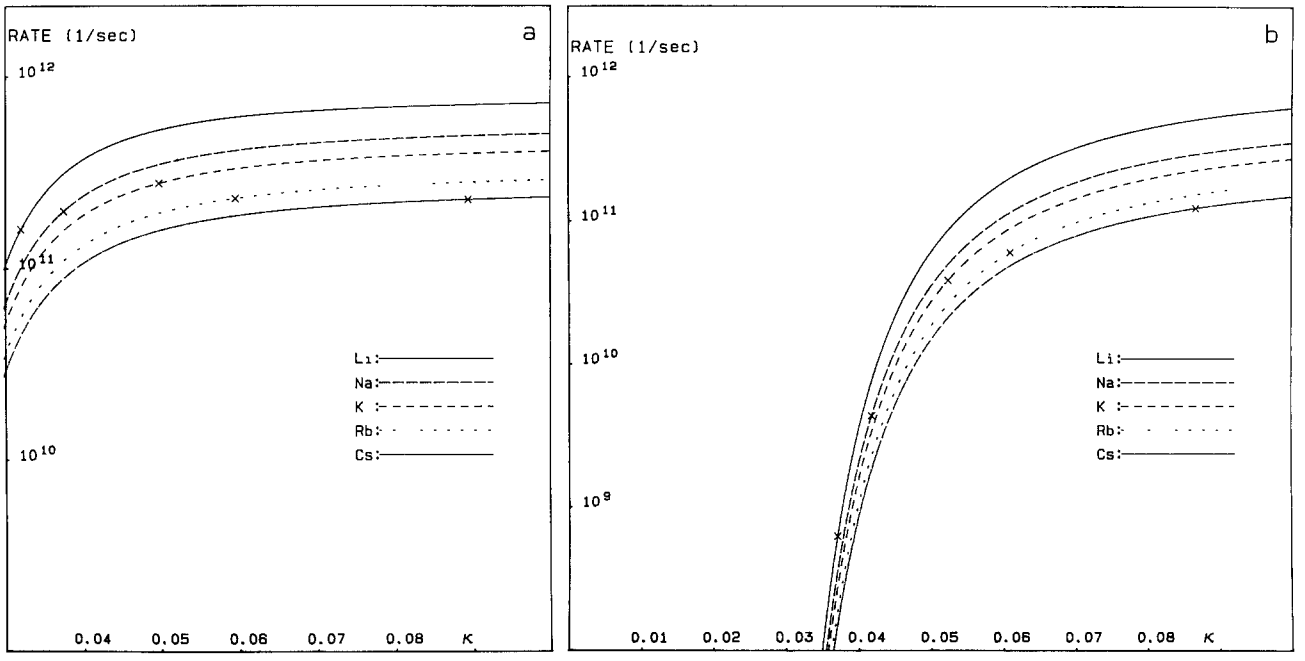

Fig. 5a. The rates presented as constant mass curves with $\varkappa$ as an independent variable for a "shoft" channel ($\varepsilon = 0.05$) at $T = 300$ K. The actual escape rates for the matching pair of mass and radius are marked by a cross on the respective constant mass curve. **b** The rates presented as constant mass curves with $\varkappa$ as an independent variable for a "hard" channel ($\varepsilon = 0.3$) at $T = 300$ K. The actual escape rates for the matching pair of mass and radius are marked by a cross on the respective constant mass curve

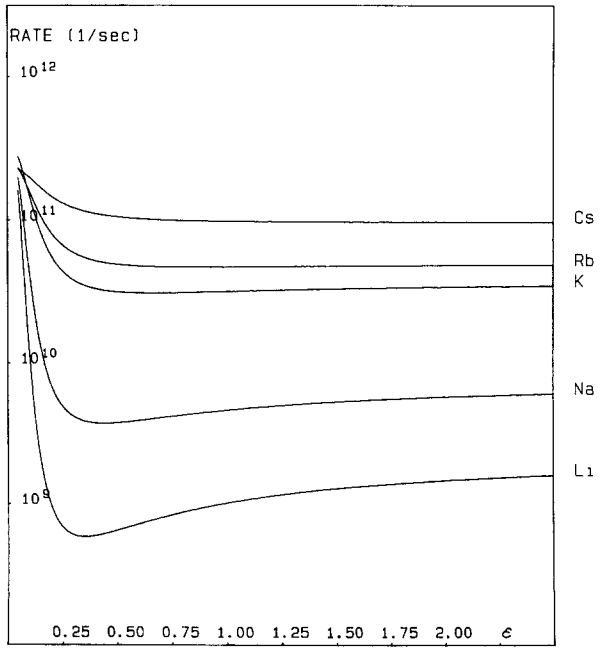

Fig. 6. The escape rates for the five different alkali ions plotted as the functions of the ligand flexibility, ε, at $T = 300$ K

ion species is automatically considered. In Fig. 6 the rates for the five alkali ions with respect to the central binding site are plotted for different values of ε ($0.05 \leqq \varepsilon \leqq 2.5$) at $T = 300$ K. For very small ε values ($\varepsilon \leqq 0.05$) the activation energies practically vanish, and therefore the application of a rate theoretical formalism is not very useful. Moreover, in this region the ligands show unrealisticly large fluctuations, because they can rotate almost without hindrance. The calculations performed down to $\varepsilon = 0.05$ have only been included to demonstrate the tendencies. Apart from this region the rates clearly follow the Eisenman sequence I with well separated values for neighbouring ions. The rates for the heavier ions Cs^+, Rb^+ and K^+ are rather insensitive to ε, whereas the lighter ions Na^+ and Li^+ are strongly affected, especially in the vicinity of small ε. This difference is a direct consequence of stronger polarization effects for smaller ions. The greatest variation among the ion specific rates are found for $\varepsilon \approx 0.3$. Coincidently in this region the librations of the ligands can be considered realistic (see Eq. (III.2)). For increasing ε the possible librations become smaller and smaller and the rates assume

asymptotically the values belonging to the rigid channel, as calculated previously (Schröder 1985). Obviously the efficiency of a channel with respect to acting ion-selectively depends essentially on the ability to perform ligand librations of a certain magnitude, here described by corresponding values of the parameter ε.

The meaning of these results must certainly be seen and discussed in the light of the experimental findings. Here the observed transmembrane currents of the gramicidin A channel are effective currents, i.e. they include effects due to the natural environment, such as water, membrane, etc. The corresponding effective conductances follow the Eisenman sequence I (Bamberg et al. 1977) with approximately the same ratios between neighbouring ions but smaller separations in comparison with the present theoretical results. Since for all binding sites within the channel a similar result as for the central binding is to be expected, the rates shown in Fig. 6 are representative for the conductance properties of the model channel in the presence of one dehydrated ion. On the other hand, the effect of additional water molecules accompanying the ion can be estimated from basic properties of the ion-channel system. It is reasonable to assume that, on the average, an ion is preceded and followed by one water molecule. Due to the mutual electrostatic interaction between ion and water this compound can be considered as a quasi-particle with an effective mass considerably larger than the ion mass. This quasi-particle is then subject to an escape process. The sandwiched ions will suffer a decrease in their mobility, where smaller ions will be more affected than larger ones. Thus the effective activation energy will be decreased more for smaller ions than for larger ones. Hence the presence of water can be expected to diminish the separation of the rates between each two neighbouring ions, where the larger ions will hardly be affected. An unchanged sequence thus requires a larger separation of neighbouring ion – specific rates in the absence of water than in the presence of water. This condition is evidently fulfilled for this model.

Summary

The subject of this investigation has been a gramicidin-like channel model with flexible ligands under the aspect of ion-specific conductance. The three-dimensional motion of the ions within the channel has been considered in the form of a paraxial approximation, where the ability to move off the channel axis has been directly related to the respective ion radius. The complex nature of the transport process due to the cross-coupling between ligand libration and three-dimensional ion motion requires an adequate rate theoretical description. For this purpose a generalized transition state method has been developed, which takes proper care of the escape across multi-dimensional barriers. It is shown that the rate with respect to a chosen reference coordinate, the reaction coordinate, is obtained from the projection of the mean reaction onto the former. The formulation of this problem leads to a renormalized expression for the rate which contains both effective mass and effective potential (potential of the mean force). Since all lattice masses are involved, the jump rate has a non-local character, i.e. the jump process between two neighbouring sites depends on the presence of all other binding sites. In the next step a detailed analysis of the equilibrium configurations and the mutually coupled motion of ion and ligands has been carried out. Thereby it has been found that the polarization effect of the channel caused by an ion strongly depends on the ion radius and on the flexibility of the ligands. For this reason small ions like Li^+ and Na^+ are generally at a disadvantage. The dwelling time of smaller ions is larger than of bigger ones. Moreover, the distance covered between two sites increases with decreasing radius in both real and configuration space. This combined effect is enhanced by the polarizability of the channel and is most pronounced when the average ligand libration is about 20°. Here the ratio of the rates between Cs^+ and Li^+ is about 200, which is 5 times larger than in the case of the rigid channel. For all reasonable values of the dipolar binding constant the model channel features a well defined Eisenman sequence I. Recent publications of Pullman et al. (Etchebest and Pullman 1984; Pullman and Etchebest 1983; Etchebest et al. 1984) concerning the energy profile of the gramicidin A channel due to the electronic polarizability of the ligands show a great similarity with the present model as far as a comparison is possible. It seems realistic to obtain a dependable simulation of the channel by a combination of both the electrostatic and the quantum-chemical model, the latter of which does not account for flexible dipoles. Since it is formally very easy to introduce an additional anisotropic polarizability for each permanent, individual dipole, the relevant quantities, i.e. effective polarizabilities could be extracted from Pullman's results and fed into an extended electrostatic model. Proceeding in accordance with the present technique the influence of the additional internal degrees of freedom on the escape rates could be studied directly.

Acknowledgement. I want to thank P. Läuger for many stimulating and encouraging discussions. This work has been supported financially by the DFG (Heisenberg-Programm).

References

Bamberg E, Alpes H, Apell H-J, Benz R, Janko K, Kolb H-A, Läuger P, Gross E (1977) Studies on the gramicidin channel. Biochemistry of Membrane Transport. FEBS Symp 42:180

Eisenman G (1967) Glass electrodes for hydrogen and other cations: Principles and practic. Marcel Dekker, New York

Eisenman G, Sandblom JP (1983) Data for gramicidin A interpreted using a single file (3B4S″) model having 3 barriers separating 4 sites. In: Spach G (ed) Physical chemistry of transmembrane ion motion. p 329

Eisenman G, Sandblom J, Neher E (1978) Interactions in cation permation through the gramicidin channel Cs, Rb, K, Na, Li, Tl, H, and effects of anion binding. Biophys J 22:307

Etchebest C, Pullman A (1984) The gramicidin A channel: II. Role of the ethanolamine end chain on the energy profile for single occupancy by Na^+. FEBS Lett 170:191

Etchebest C, Ranganathan S, Pullman A (1984) The gramicidin A channel: Comparison of the energy profiles of Na^+, K^+ and Cs^+. FEBS Lett 173:301

Hille B (1975) Ionic selectivity, saturation, and block in sodium channels. A four-barrier model. J Gen Physiol 66:535

Kramers HA (1940) Brownian motion in a field of force and the diffusion model of chemical reactions. Physica 7:284

Läuger P (1973) Ion transport through pores: A rate-theory analysis. Biochim Biophys Acta 311:423ff

Läuger P (1979) Transport of non interacting ions through channels. In: Stevens CF, Tsien RW (eds) Membrane transport processes, vol 3. Raven, New York, pp 17ff

Levitt DG (1978a) Electrostatic calculations for an ion channel: I. Energy and potential profiles and interactions between ions. Biophys J 22:209

Levitt DG (1978b) Electrostatic calculations for an ion channel: II. Kinetic behavior of the gramicidin A channel. Biophys J 22:221

Pullman A, Etchebest C (1983) The gramicidin A channel: I. The energy profile for single and double occupancy in a head-to-head $\beta^{6}_{3},^{3}_{3}$-helical dimer backbone. FEBS Lett 163:199

Schröder H (1983a) Transit time conception for ion diffusion through membrane channels. J Chem Phys 79:1991

Schröder H (1983b) Rate theoretical analysis of ion transport in membrane channels with elastically bound ligands. J Phys Chem 79:1997

Schröder H (1983c) Rate theoretical analysis of ion transport in membrane channels with elastically bound ligands. In: Spach G (ed) Physical chemistry of transmembrane ion motions. Elsevier, Amsterdam, p 425

Schröder H (1984) Model calculations of polarization effects in elastic membrane channels. Biophys Chem 20:157

Schröder H (1985) A molecular model for ion selectivity in membrane channels. Eur Biophys J 11:157

Schröder H, Brickmann J, Fischer W (1983) Cation transport through biological transmembrane channels, theoretical studies of mass dependent anomalies in the diffusion constant. Mol Phys 49:973

Urry DW (1971) The gramicidin A transmembrane channel: A proposed $\pi_{(L,D)}$ helix. Proc Natl Acad Sci USA 68:672

Urry DW, Goodall MC, Gliekson JD, Mayers DF (1971) The gramicidin A transmembrane channel: Characteristics of head-to head dimerized $\pi_{(L,D)}$ helices. Proc Natl Acad Sci USA 68:1907

Vineyard GH (1957) Frequency factors and isotope effects in solid state rate processes. J Phys Chem Solids 3:121

Weidenmüller HA, Zhang Jin-Shang (1984) Stationary diffusion over a multidimensional potential barrier: A generalization of Kramer's formula. J Stat Phys 34:191

Woodbury JW (1971) Eyring rate theory model the current-voltage relationship of ion channels in excitable membranes. Chemical Physics, Papers in Honor of Henry Eyring (Hirschfelder J, ed), p 601